J Am Oil Chem Soc (2011) 88:223–233
DOI 10.1007/s11746-010-1665-z

ORIGINAL PAPER

Phase Equilibrium and Optimization Tools: Application for Enhanced Structured Lipids for Foods

Moises Teles dos Santos · Galo A. C. Le Roux · Vincent Gerbaud

Received: 1 April 2010 / Revised: 30 June 2010 / Accepted: 30 July 2010 / Published online: 19 August 2010

Abstract Solid–liquid phase equilibrium modeling of triacylglycerol mixtures is essential for lipids design. Considering the α polymorphism and liquid phase as ideal, the Margules 2-suffix excess Gibbs energy model with predictive binary parameter correlations describes the non ideal β and β' solid polymorphs. Solving by direct optimization of the Gibbs free energy enables one to predict from a bulk mixture composition the phases composition at a given temperature and thus the SFC curve, the melting profile and the Differential Scanning Calorimetry (DSC) curve that are related to end-user lipid properties. Phase diagram, SFC and DSC curve experimental data are qualitatively and quantitatively well predicted for the binary mixture 1,3-dipalmitoyl-2-oleoyl-*sn*-glycerol (POP) and 1,2,3-tripalmitoyl-*sn*-glycerol (PPP), the ternary mixture 1,3-dimyristoyl-2-palmitoyl-*sn*-glycerol (MPM), 1,2-distearoyl-3-oleoyl-*sn*-glycerol (SSO) and 1,2,3-trioleoyl-*sn*-glycerol (OOO), for palm oil and cocoa butter. Then, addition to palm oil of Medium-Long-Medium type structured lipids is evaluated, using caprylic acid as medium chain and long chain fatty acids (EPA-eicosapentaenoic acid, DHA-docosahexaenoic acid, γ-linolenic-octadecatrienoic acid and AA-arachidonic acid), as *sn*-2 substitutes. EPA, DHA and AA increase the melting range on both the fusion and crystallization side. γ-linolenic shifts the melting range upwards. This predictive tool is useful for the pre-screening of lipids matching desired properties set a priori.

Keywords Triacylglycerols · Structured lipids · Solid–liquid equilibrium · DSC · Solid fat content · Melting point · Medium chain fatty acid · Long chain fatty acid

M. T. dos Santos · G. A. C. Le Roux
Escola Politécnica, Laboratório de Simulação e Controle de Processos, Universidade de São Paulo, Av. Prof. Lineu Prestes, São Paulo 5088-900, Brazil

M. T. dos Santos · V. Gerbaud
INP, UPS, LGC (Laboratoire de Génie Chimique), Université de Toulouse, 4 allée Emile Monso, 31030 Toulouse Cedex 04, France

M. T. dos Santos · V. Gerbaud (✉)
LGC (Laboratoire de Génie Chimique), CNRS, 31030 Toulouse Cedex 04, France
e-mail: Vincent.Gerbaud@ensiacet.fr

List of symbols

ΔH	Enthalpy (kJ/mol)
ε	Degree of isomorphism
γ	Activity coefficient
μ	Chemical potential (kJ/mol)
a, A	Binary interaction parameters
C_p	Molar heat capacity (kJ/mol)
G	Extensive Gibbs free energy (kJ)
G	Molar Gibbs free energy (kJ/mol)
$\overline{g}$	Partial molar Gibbs free energy (kJ/mol)
H	Extensive enthalpy (kJ)
n	Number of moles
P	Pressure (bar)
q	Molecule size parameter
R	Gas constant (kJ/mol K)
S	Specific entropy (kJ/mol K)
T	Temperature (K)
V	Molar volume (cm^3/mol)
v_0	Sum of the carbon number
v_{non}	Absolute difference in carbon number
X	Molar fraction

Subscripts

i	Component i
o	Pure state

m Melting state

Superscripts

j Solid phase j
nc Number of components
np Number of phases
E Excess property
ap Apparent
p Phase p

Introduction

The so-called functional foods represent an expanding market and food functionalizing is a major factor driving the development of new products [1]. Fat-based foods are composed mainly by triacylglycerols (TAG), a class of lipids responsible for more than 95% of composition in fats and oils. Such molecules have a large application in the food industry: they are important sources of energy, essential fatty acids, fat-soluble vitamins and they impart flavor, texture and palatability to foods [2]. When determining the suitability of novel lipids for use in food applications, physico-chemical properties of fat-based products such as improved spreadability, a specific melting point, a particular solid fat content (SFC) at a given temperature, melting profiles (SFC curves), precise rheological behavior and crystal habit are as fundamental as texture, appearance or nutritional properties [3]. Acknowledging the expertise of food makers, matching these physico-chemical end-user properties often remains an empirical recipe in practice and more systematic (computer-based) approaches, as we consider in this manuscript, can be useful for evaluating triacylglycerols mixtures in a pre-experimental step.

Bulk physiochemical properties and sensory attributes of many fatty foods are determined by the fraction of the fat phase that is solidified at a particular temperature, namely the SFC curve [4]. Fat-based food products used as bakery shortening enhancers can be described mainly by seven sensory attributes: color, texture, moistness, oiliness, denseness, taste and aroma, and principal component analysis has shown that color, SFC, melting temperature, aroma and denseness are the main factors enabling us to discriminate among products [5].

Taste is strongly correlated with melting temperature and SFC perception in the mouth [3, 5]: fats should be completely melted at 36 °C and SFC contributes to the cooling sensations of a product in the mouth. In margarines, a large difference between the SFC at 15 °C and 25 °C is correlated to increased cooling sensations [3]. In baking shortenings, optimal performance is achieved with an SFC between 15 and 25% at the usage temperature whereas an excess of liquid can cause an oiliness sensation decreasing scores of sensorial attributes [5].

Considering the available experimental information, phase diagrams, differential scanning calorimetry (DSC) curves, SFC melting curves and fatty acid distributions are found, delivering information of varying interest. One rarely finds fat phase diagrams that report the clear and softening points. The clear point is the temperature at which the last solid phase disappears (completely fusion) and the softening point is the temperature at which the last liquid phase disappears (complete crystallization). On the other hand, DSC curves are often a readily available measurement that can display solid phase transitions; quite clearly for simple TAG or fatty acid systems but hardly readable for oils.

The fat complete melting point gives limited information on the fat consistency. Indeed, fats with the same final melting point can have widely different consistencies at room temperature. On the other hand, a SFC curve describes the whole melting profile of a fat and can also be correlated with sensory attributes such as hardness [6, 7].

The fatty acid distribution is often measured but it is not straightforward to relate it to the SFC and therefore to end-user properties. A reason is that oils are mixtures of triacylglycerols, with each of the triacylglycerols (TAG) bearing three fatty acids, and that each TAG can crystallize in several polymorphic forms, each with its own melting point.

So-called Structured Lipids (SLs) are defined as lipids restructured by chemical or enzymatic processes to change their fatty acid composition and/or the stereochemical positions of fatty acids on the glycerol backbone. Among the possible improvements sought are specific metabolic effects, nutritive or therapeutic purposes, physical and/or chemical characteristics of lipids [8]. MLM (medium-long-medium) and CLA (conjugated linoleic acids) triacylglycerols are recognized for their improved nutritional characteristics [9]. MLM has medium chain fatty acids (MCFA) (C6-C12) in stereo positions *sn*-1 and *sn*-3 of the glycerol backbone and functional long-chain polyunsaturated fatty acids (PUFA) in position *sn*-2. The CLA is a general term for the positional and geometric isomers of octadecadienoic acid with conjugated double bonds at carbon atoms 9/11 or 10/12 [9].

MLM molecules utilize the benefits of the fast energy provided by the medium-chain fatty acid (specially caprylic, capric, caproic and lauric acids) and the nutritional effects of long-chain fatty acid, especially EPA (5,8,11,14,17-eicosapentaenoic acid–C20:5), DHA (4,7,10,13,16,19-docosahexaenoic acid–C22:6), γ-linolenic acid (6,9,12-octadecatrienoic acid–C18:3) and AA (arachidonic acid–C20:4) [9].

MCFA have several desired features such as high oxidative stability (due to their saturation), low viscosity and melting points and high solubility in water. They also provide quick energy and fast absorption without significant

tendency to accumulate in the fat tissues [8]. As MCFA alone cannot provide essential fatty acids, they are combined with long chain fatty acids (LCFA) for better nutritional purposes, not achieved by physical mixture of long chain and medium chain fatty acids [10].

The LCFA, like the famous omega-3, polyunsaturated fatty acids have been recognized for their important role in health: EPA can reduce the level of very low density lipoprotein (VLDL) and low-density lipoprotein (LDL) cholesterol in humans and can help to prevent arteriosclerosis and thrombosis. DHA is important for brain development and the retina [11, 12].

Therefore, positioning medium-chain fatty acids in the *sn*-1 and *sn*-3 position of the glycerol backbone imparts fast absorption of these acids in the body while unsaturated long-chain fatty acids in the *sn*-2 position may increase the nutritional value of the molecules involved.

The number of possible tailor-made TAG rapidly increases with the number of fatty acids considered (see Fig. 1), as different sets composed by three fatty acids can be used and, for a given set, many positional isomers can be formed. Together with the consideration of the final mixture composition and number of TAG present as variables, the problem size becomes impossible to handle experimentally.

The present work concerns the validation of a predictive solid–liquid equilibrium algorithm by direct minimization of Gibbs Free Energy. It enables us to evaluate how molecular structure and mixture composition affect final properties such as SFC and melting profiles suitable for hinting at the recipe directions that must be investigated to achieve enhanced chemical structures for nutritional purposes while satisfying consumers sensorial requirements. This work fits in our scope of computer aided product design (CAPD) for structured lipids where target properties of various kinds (SLE-related properties as dealt with here, nutritional power, viscosity properties, etc.) are set as the objective of a reverse engineering problem and many candidate mixtures of oils and value added TAG are evaluated by predictive tools with respect to these target properties [13].

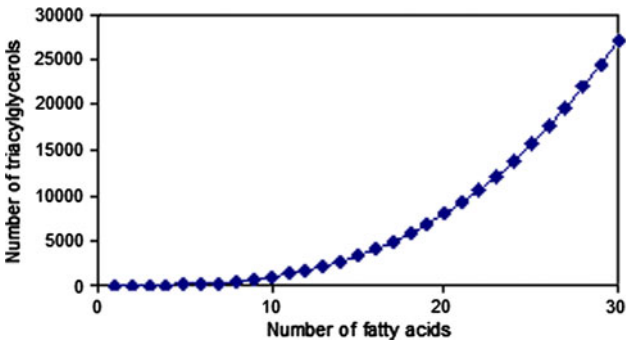

Fig. 1 Number of triacylglycerols that can be formed from fatty acids (including optical and positional isomers)

First, the solid–liquid equilibrium principles are described in the light of TAG application and former modeling works are recalled before selecting a model suitable for a predictive tool. Second, the solving scheme based on optimization is presented along with a synthesis of robustness and numerical issues. Third, the predictive model is validated, without any fitting, on selected systems for which experimental data is available, first on binary and ternary TAG mixtures, then on multi-component vegetable oils (palm oil and cocoa butter). Finally, structured lipids for which there are no experimental data as mixtures of palm oil supplemented with value-added MLM TAG are considered, in order to investigate how the added TAG affect their melting curves. Table 1 summarizes the mixtures used in this work.

Methods

Background on Fat Thermodynamic Equilibrium Modeling

Due to their high molecular weight, TAG tend to crystallize in a solid network with different crystals packing called polymorphisms. The most common are the unstable α-form (least dense crystal packing), the metastable β'-form and the stable β-form (most dense crystal packing)

Table 1 Type of mixtures used

Binary mixture	Ternary mixture	Multicomponent mixtures (vegetable oils)	Blends of vegetable oils and structured lipids
POP/PPP	MPM/SSO/OOO	Palm oil	Palm oil + (Caprylic–EPA–Caprylic)
		Cocoa butter	Palm oil + (Caprylic–DHA–Caprylic)
			Palm oil + (Caprylic–γ linolenic–Caprylic)
			Palm oil + (Caprylic–AA–Caprylic)

P palmitic acid (C16:0), *O* oleic acid (18:1), *M* myristic acid (C14:0), *S* stearic acid (18:0), *EPA* eicosapentaenoic acid (C20:5), *DHA* docosahexaenoic acid (C22:6), *AA* arachidonic acid (C20:4), *γ-linolenic acid* 6,9,12-Octadecatrienoic acid (C18:3)

[14]. Polymorphic forms are distinguished by their own temperature of fusion and enthalpy of fusion and they impact SFC and DSC curves which are indeed used experimentally to explore the polymorphic behavior of fats.

SFC computation until 1990 was mainly empirical, partially based on curve fitting [15]. After 1990, the literature mostly published experimental studies [16–18] and some equilibrium modeling issues [19–22]. Won [20] used iterative methods to compute softening and clear points with no considerations about computing activity coefficients on solid and liquid phases and applied it to cocoa butter.

There are mainly three solid–liquid equilibrium models that have been used in the current literature for fatty mixtures: Bragg–Williams approximation [23], Slaughter and Doherty model [24] and Margules-isomorphism correlations [15, 19]. The Bragg–Williams approximation assumes non-ideal mixing in both liquid and solid phases and attributes the non-ideality of mixing to the enthalpy term of the free energy of mixing, supposing that the entropy term is like in the ideal mixing. It uses parameters which are the energy difference between molecules pairs in solid and liquid phases, fitted to experimental binary data [25, 26]. The Slaughter and Doherty model deals with solid compound-forming systems, like stoichiometric peritectic compounds in the solid phase and considers that the solid phases are almost immiscible. Seven binary fatty acid mixtures were also studied with the Slaughter and Doherty model for the solid phase while testing the Margules-2-suffix, Margules-3-suffix, UNIFAC modified Dortmund 93, and NRTL thermodynamic excess Gibbs free energy models to compute the liquid activity coefficients [22]. Fitting those model parameters to experimental data, the authors concluded that the combination of the Slaughter–Doherty model for solid and the Margules-3-suffix model for liquids achieved the best reproduction of the experimental data. Concerning the Margules-isomorphism model, a large experimental data collection was examined and it was noted that Margules interaction parameters in the β' and β solid phases were reasonably correlated to the degree of isomorphism between two molecules [15]. Application of the Flory–Huggins theory led them to consider the liquid phase as ideal in most cases, except when large difference in molecular size (differences in carbon numbers greater than 15–20) occurs among the TAG [15]. They also concluded that solid non ideality comes from substantial distortion in the regular crystal lattice of a pure component by adding a molecule of another size and that distortion is non significant in a disordered state as α polymorph but must be accounted for in the denser packed β' and β systems.

After analysis of these previous works, we selected the Margules model [27] in the present work, as it is well-suited for mixtures whose components have similar molar volumes, shape and chemical natures. Also, the isomorphism correlation for the Margules binary interaction parameters will be used because they serve our goal of running predictive simulations without fitting any parameter on experimental data within the context of CAPD reverse formulation.

Despite the occurrence of other fat solid polymorphism such as γ and of sub-forms such as $\beta 2$ and $\beta 3$ [15], we only consider the α, β and β' solid phases possible in equilibrium with a liquid phase, as there are no predictive models to calculate melting temperature and melting enthalpy in other forms and experimental data are very scarce.

The Margules model and the isomorphism correlations are detailed in Appendix.

Solid–Liquid Equilibrium Modeling of Fats

The condition for thermodynamic equilibrium is that the chemical potential of each component i in each phase must be equal to that in any other phase. For a liquid phase in equilibrium with at least one solid phase j,

$$\mu_i^{liquid} = \mu_i^{solid(j)} \tag{1}$$

or

$$\mu_{i,0}^{liquid} + RT\ln(\gamma_i^{liquid} x_i^{liquid}) = \mu_{i,0}^{solid(j)} + RT\ln(\gamma_i^{solid(j)} x_i^{solid(j)}) \tag{2}$$

For the chemical potential of molecule i in the reference state:

$$d\mu_{i,0}^{p} = -S_{i,0}^{p} dT + V_{i,0}^{p} dP \tag{3}$$

where:

$$\Delta S_{i,0} = \Delta H_{i,0}/T \text{ and } \Delta H_{i,0} = \Delta H_{m,i,0} + \Delta C_{p,i,0}(T - T_{m,i}) \tag{4}$$

The effect of pressure in condensed phases such as solids and liquid can be neglected at pressures that are not too high. Assuming $\Delta C_{p,i}$ to be independent of temperature, after some rearrangements Eq. (1) can be rewritten as:

$$\ln\left(\frac{\gamma_i^{solid(j)} x_i^{solid(j)}}{\gamma_i^{liquid} x_i^{liquid}}\right) = \frac{\Delta H_{m,i}^{solid(j)}}{R}\left(\frac{1}{T} - \frac{1}{T_{m,i}^{solid(j)}}\right) - \frac{\Delta C_{p,i}}{R}\left(\frac{T_{m,i}^{solid(j)} - T}{T}\right) + \frac{\Delta C_{p,i}}{R}\ln\frac{T_{m,i}^{solid(j)}}{T} \tag{5}$$

Solid–liquid equilibrium can also be formulated in terms of the Gibbs free energy that must be minimal at

equilibrium. The intensive Gibbs free energy for a phase p is:

$$g^p = \sum_{i=1}^{nc} x_i^p (\mu_{i,0}^p + RT \ln \gamma_i^p x_i^p) \quad (6)$$

For TAG systems $\Delta C_p = 0.2$ kJ/mol and the difference (T_m–T) is never greater than 70 K (usually between 0–20) [15]. Together with setting the chemical potential in the pure liquid reference state to zero, this enables us to simplify Eq. (6) and write for the liquid phase molar Gibbs free energy:

$$g^{liquid} = RT \sum_{i=1}^{nc} (x_i^{liquid} \ln x_i^{liquid}) \quad (7)$$

and for p being one of the possible solid phases (α, β' or β):

$$g^p = RT \sum_{i=1}^{nc} x_i^p \left(\frac{\Delta H_{m,i}^p}{R} \left(\frac{1}{T} - \frac{1}{T_{m,i}^p} \right) + \ln \gamma_i^p x_i^p \right) \quad (8)$$

Solving the Solid–Liquid Equilibrium by Direct Minimization of Gibbs Free Energy

Computing the phase equilibrium is the solution of a nonlinear programming problem searching for the global minimization of the Gibbs free energy G, subject to material balance constraints written as an equivalent set of nonlinear equations:

$$\begin{aligned} \min \; G(n) &= \sum_{i=1}^{nc} \sum_{j=1}^{np} n_i^j \mu_i^j(n) = \sum_{j=1}^{np} n^j g^j \\ & \qquad s.t. \\ n_i &= \sum_{j=1}^{np} n_i^j \quad i = 1 \ldots nc \\ 0 \le n_i^j &\le n_i \; i = 1 \ldots nc; \quad j = 1 \ldots np \end{aligned} \quad (9)$$

The solution of the solid liquid equilibrium gives the number of phases, the fraction of each phase and their composition. When spanning a temperature range, the total solid content, SFC and DSC curves can be computed.

One of the main difficulties associated with minimizing the Gibbs free energy is the a priori determination of the number of phases. If too few phases are allowed, then convergence to constrained minima can occur; if too many are assumed, then numerical problems may arise like Jacobian matrix singularities in Newton-based methods, or convergence to trivial or local extrema may occur [28]. In a previous work, we succeeded in solving the SLE for several nine TAG mixtures in a two step approach: first solving the stability tests and second computing the equilibrium compositions [29]. The Michelsen method [30] for stability analysis was adapted to cope with polymorphisms and was successful for phase-split detection but revealed itself to be initialization dependent and failed in detecting phase splitting for some mixtures. To overcome this limitation, the present work deals with the direct minimization of Gibbs Free Energy using a Generalized Reduced Gradient (GRG) method available in the GAMS software [31] considering a priori a sufficient number of phases to be present, namely nine solid phases plus a liquid in our case. After some initial evaluations of the performance of the available optimizers, CONOPT3 was chosen among six others as it showed the best relation time/accuracy in finding exact solutions for selected mixtures of known results. Solving the palm oil example ten times with 17 TAG over 79 temperatures (2,370 optimization problems) was achieved in 31 s with 0/79 failures. The second best available optimizer based on a branch-and-cut method, had a mean failure of 8/79 and required more than a 300 times more time, whereas its accuracy in terms of minimum Gibbs free energy value was 0.01% higher than those obtained with CONOPT3.

To summarize the calculation section, the bulk mixture composition in TAG is an input as well as the temperature of calculation. Then nine solid phases plus one liquid phases are supposed initially to co-exists with TAG split randomly between the initial phases. The Gibbs free energy optimization predicts the number of coexisting phases and their TAG composition along with their Gibbs free energy value and the total Gibbs free energy value. The SFC curve is then readily computed from this information by sequentially increasing the temperature of the mixture until there is no more solid present.

Differential Scanning Calorimetry Curve Simulation

A DSC curve is related to apparent heat capacity which can be computed from the following equations [32]:

$$C_p^{ap} = C_p + \left(\frac{\partial H}{\partial T} \right)_n \quad (10)$$

Also, the excess enthalpy and excess Gibbs energy are given by:

$$H^E = H - \sum_{j=1}^{np} \sum_{i=1}^{nc} n_i^j H_{i,0}^j \quad (11)$$

$$G^E = H^E - TS^E \quad (12)$$

Setting reference enthalpy to zero on liquid state, H_0 for any i specie on phase j in Eq. 11 becomes the melting enthalpy of that solid phase. Thus:

$$H_{i,0}^j = \Delta H_{m,i}^j \quad (13)$$

Assuming that triacylglycerols solid mixtures are regular solutions (excess entropy equals to zero), $H^E = G^E$ and an

expression for H can be put from Eq. 11 into Eq. 10 to compute the apparent heat capacity taking into account the solid transitions:

$$C_p^{ap} = C_p + \frac{\partial G^E}{\partial T} + \sum_{j=1}^{np}\sum_{i=1}^{nc} \Delta H_{m,i}^{j} \frac{\partial n_i^j}{\partial T} \quad (14)$$

Equation 14 shows that for each point on the DSC curve, the apparent heat capacity can be calculated by using two derivatives, which in turn can be obtained by numerical differentiation of SLE results (excess Gibbs energy and number of moles) at two different temperatures (T_i and $T_i + \Delta T$).

The DSC simulated curves are then calculated with the hypothesis that chemical equilibrium has been reached; which may rarely be the case for all experimental DSC curves that are cooling/heating rates dependent.

Pure component properties needed for computing SFC curves from SLE are the melting temperature (T_m), the melting enthalpy (H_m) to which is added the heat capacity (C_p) for DSC curves. Whenever possible, the experimental data bank for T_m and H_m for different polymorphism for different TAG was used [15]. But in the context of CAPD reverse formulation, we have also used temperature and enthalpy of fusion correlations based on carbon number, number of double bounds, position of fatty acids in the molecule and asymmetry [15] or a group interaction contribution model for saturated TAG that accounts for isomerism [33]. For heat capacity, we used a recently published group contribution method regressed over 1,395 values for 86 types of fatty compounds (saturated and unsaturated FA, fatty esters, fatty alcohols, saturated and unsaturated TAG and hydrocarbons) [34]. The reader should consult the references cited for further details.

Results and Discussions

Binary Mixture (Palmitic-Oleic-Palmitic/Palmitic-Palmitic-Palmitic)

Solid–liquid T,x,y phase diagram experimental data [35] for the binary mixture Palmitic-Oleic-Palmitic (POP) and Palmitic-Palmitic-Palmitic (PPP) are compared in Fig. 2 with the simulated results. The TAG crystals are in the β form (no submodifications $\beta 2$ or $\beta 3$ of the β class are considered in this work). The solid line (softening points) and liquid line (clear points) with a large region of coexistence solid–liquid for the whole range of POP fraction can be seen.

Predictions agree better with the liquid phase line than with the solid phase line, especially for POP-lean mixtures. Although deceptive, these results are in accordance with previous literature results [15]: according to those authors,

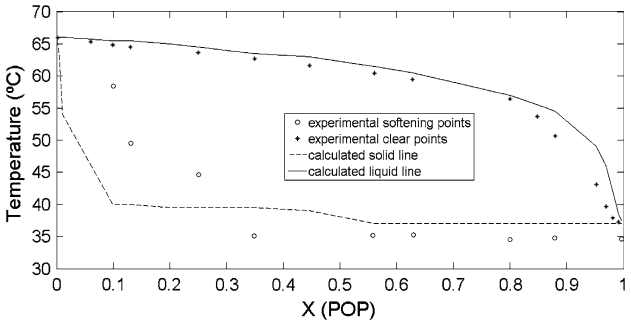

Fig. 2 Experimental and predicted phase diagram for mixture POP-PPP

this is related to the fact that the visual observations of clear and specially softening points are very inaccurate. Also, impurities can increase the melting points and incomplete stabilization due to extremely low diffusion rates in solid phase can lead to imprecision in determining the initial temperature of fusion and thus the solid phase line location.

In the POP-rich region, the increasing presence of the unsaturated oleic chain, well known for its very low melting point near 14 °C, lowers the TAG mixture melting range.

Ternary Mixture (Myristic-Palmitic-Myristic/Stearic-Stearic-Oleic/Oleic-Oleic-Oleic)

The SFC-temperature curve is computed for the ternary-mixture Myristic-Palmitic-Myristic (MPM), Stearic-Stearic-Oleic (SSO) and Oleic-Oleic-Oleic (OOO) with mass composition 25, 25, and 50%, respectively (Fig. 3a). Then the DSC curve is computed from Eq. (14) and compared in Fig. 3b with experimental data in the β' modification obtained at 1.25 °C/min after a 3 day stabilization time [15]. They are in good quantitative and qualitative agreement.

In this mixture, the triolein (OOO) TAG (melting point −10 °C), is used as a "liquid solvent" to increase the

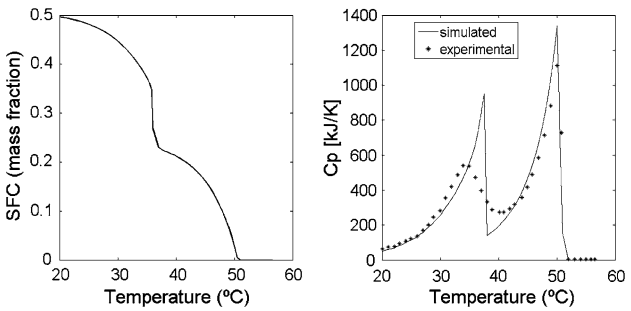

Fig. 3 Simulated SFC versus Temperature and simulated and experimental DSC for mixture MPM/SSO/OOO

diffusion rates of MPM and SSO in the solid phase. The model correctly detected that at the start temperature of 17 °C all the OOO TAG (50% of the mixture composition) is in the liquid phase, in agreement with the experimental observation. It must be highlighted that at the initial temperature, the computer tool randomly distribute the molecules in the phases, and then the solver converges to a solution. In the MPM/SSO/OOO case, despite an initial random amount of OOO in the solid phase being non-zero, the method correctly converged to a zero amount of solid OOO.

The DSC curve displays two peaks. The first one is the endothermic peak caused by fusion of SSO (experimental $T_m = 41.9$ °C) and the second one is due to the MPM fusion (experimental $T_m = 59.5$ °C). That curve with distinct melting peaks is typical for mixtures where the molecules are well-distinguished one from another in shape and size. The low isomorphism (0.77) of such a mixture is responsible for its non ideal behavior. One also notes that the transition temperatures in the mixture (Fig. 3b) do not correspond to the pure compound temperature transitions as the mixture deviates from ideal behavior.

Pure Palm Oil

Computation for palm oil is another step in the computer tool validation. Palm oil currently accounts for 13% of the total world production of oils and fats and is expected to overtake soybean oil as the most important vegetable oil. Almost 90% of the world palm oil production is used as food [36].

In this work, the palm oil was modeled by 17 TAG corresponding to 91.56% in weight of the palm oil composition (Table 2). Data about the TAG type and composition was taken from literature [36] and minor components (TAG and other molecules) with very low fraction or not available/computed pure properties were discarded. None of these minor components are responsible for more than 0.83% of overall composition. Only the TAG explicited in Table 2 were considered in the calculations, after renormalization.

Lin [37] recorded the SFC at seven temperatures for 244 samples of palm oils of various origins. The SFC computed from the renormalized composition of Table 2 is compared to the mean experimental points [37] in Fig. 4a. Figure 4b shows the related DSC simulation for this vegetable oil. We did not compare this to other models for palm oil as we could not find in the literature any other melting range calculation using modeling.

Figure 4a shows that despite some discrepancy, the SFC curve shape agrees with the experimental data: the final melting points are alike; from 10 °C to 20 °C both simulated and experimental data display a steep slope, while from 25 °C to 40 °C the slope is more gradual. Overall, the mean difference over the 10–40 °C range between the calculated and experimental SFC value is 8.2%. The predicted SFC curve also indicates that there is only a solid at −20 °C. It can also determine the solid fraction at any intermediate temperature, giving useful information for product design requirements.

Looking at the DSC curve, its shape is typical for mixtures with a high number of molecules. The number of peaks is different from the number of molecules, 17 TAG, because peaks for molecules with close transition temperatures overlap. As pointed out in the literature [38], these peaks are not easily interpretable, depend on heating/cooling rates and on entire thermal history of the sample.

Table 2 Weight fraction of pure palm oil and cocoa butter

Palm oil [36]		Cocoa butter [39]	
TAG	Mass fraction (%)	TAG	Mass fraction (%)
POO	20.54	POS	40.2
POP	20.02	SOS	21.7
PPO	7.16	POP	13.9
PPP	6.91	SOO	6.7
PLO	6.59	POO	5.8
PLP	6.36	PLS	3.9
OOO	5.38	PLP	1.7
POS	3.5	PLO	0.9
POL	3.39	OOO	0.7
OPO	1.86	PPS	0.6
SOO	1.81	SSS	0.6
OOL	1.76	PSS	0.5
OLO	1.71	–	–
PPS	1.21	–	–
PPL	1.17	–	–
PLS	1.11	–	–
PLL	1.08	–	–
Others	8.44		2.8
Total	100	–	100

P palmitic, *O* oleic, *L* linoleic, *S* stearic

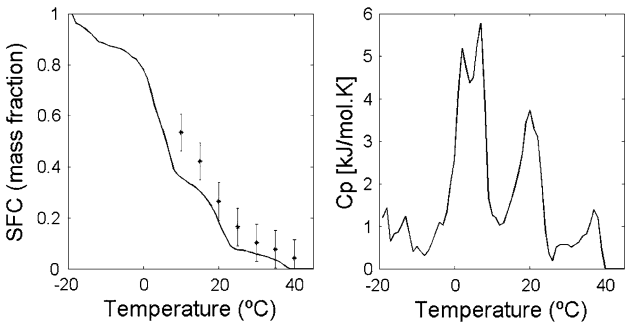

Fig. 4 Melting profile and DSC curve of palm oil. Calculated *full lines*. Experimental data *symbols* [37]

Experimental DSC curves are scan rate, temperature programming and stability procedure dependent (which leads to experimental curves with different shapes) and numerous thermal transitions and thermal lag can occur [38]. Thus, it is difficult to choose what experimental curve must be considered. Actually, comparing simulated DSC generated by ESL results and experimental DSC curves is not suitable, unless the experimental data were judiciously conducted in order to achieve equilibrium, as is the case for Fig. 3b. However, a simulated DSC curve reveals the heat capacity change of the sample due to state transitions, indicating the temperatures where the most accentuated changes occur.

Cocoa Butter

Cocoa butter is the only natural fat melting sharply just below mouth temperature, leaving a clean, cool, non-greasy sensation on the palate [6]. Its unique and specific TAG composition (Table 2) is responsible for these highly desired sensory properties. In chocolates, a sharp melting point is a sign of intense cooling sensations in the mouth [3]. Therefore, reducing the tail of the SFC vs temperature curve is a must sought for feature in industry to improve mouth feel in cocoa butter equivalents (CBE), cocoa butter replacer (CBR) and cocoa butter substitutes (CBS).

Cocoa butter SFC experimental data was taken from one source in the literature [20] and the TAG composition was taken from another [39]. The composition reported in Table 2 shows that 12 saturated and unsaturated TAG are used to represent cocoa butter (97.2% weight), discarding minor components accounting for 2.8% weight. Compositions are renormalized before calculation.

Figure 5 shows that the model predictions are consistent with experimental data in terms of melting profile shape, but the final melting temperature is over predicted by more than 10 °C. Overall, quantitative agreement was achieved within less than 15%, a fair value considering that we did not perform any fitting. Other causes of discrepancy are the fact that the experimental data were not obtained by the authors who provided the compositions used for the prediction; the compositions for prediction discard 2.8% in weight of the measured composition.

Comparing cocoa butter and palm oil, cocoa butter has a melting range around 30 °C, half that of palm oil around 60 °C. The cocoa butter DSC predictions shows broader and less numerous peaks, corresponding to more solid–liquid molecular transitions over similar temperatures.

Prediction of Palm Oil Enriched with Structured Lipids (SLs)

The aim of the present algorithm is that it can be used in a predictive manner and we can simulate the effects of adding highly unsaturated MLM molecules on the melting profile of pure palm oil.

First, the molecule Caprylic–EPA–Caprylic (caprylic–eicosapentaenoic acid–caprylic), a structured lipid of type MLM is added to palm oil in 6 different concentrations (5, 10, 20, 30, 40 and 50%). Figure 6 represents the melting curves for these mixtures whereas Fig. 7 shows the related DSC curves

Figure 6 shows that the addition of Caprylic–EPA–Caprylic affects strongly the palm oil melting curve even at low concentrations. Pure palm oil is solid at −20 °C, but

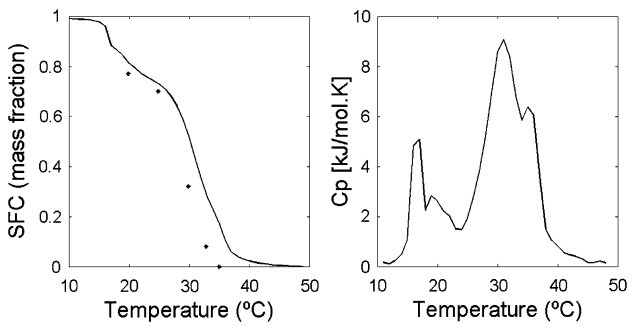

Fig. 5 Melting profile and DSC curve of cocoa butter. Calculated *full lines*. Experimental data *symbols* [20]

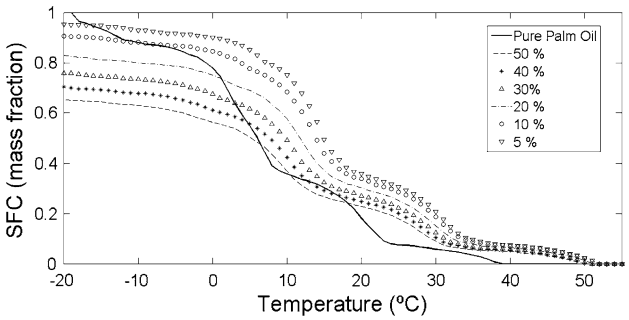

Fig. 6 Simulated melting curves for palm oil enriched with Caprylic–EPA–Caprylic structured lipid (different concentrations) compared with the melting curve for pure palm oil

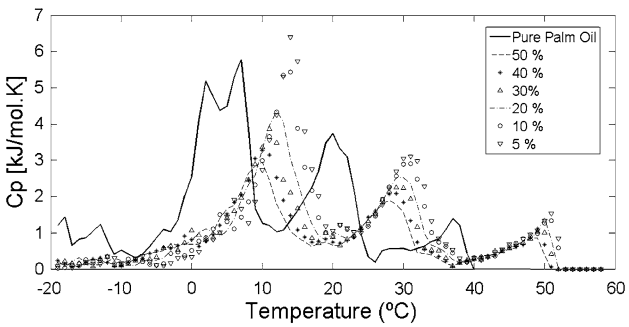

Fig. 7 Simulated DSC curves for the mixtures presented in Fig. 6

5% Caprylic–EPA–Caprylic already imposes some liquid content at −20 °C. This is expected as Caprylic–EPA–Caprylic has a very low melting point due to its five unsaturations. As Caprylic–EPA–Caprylic concentration increases, the SFC decreases significantly at −20 °C, reaching 65% SFC for 50% of Caprylic–EPA–Caprylic. However, the benefit of lowering the SFC of palm oil is not kept for the whole melting range. Indeed, the Caprylic–EPA–Caprylic enriched curves cross the pure palm oil curve and pure palm oil becomes completely melted before the Caprylic–EPA–Caprylic enriched oil. As a whole, the enriched oils have an extended melting range on both sides, with a final melting point increased by about 11 °C ($T_m = 51$ °C) for all concentrations between 5 and 50%.

Figure 7 shows the DSC simulations for the enriched palm oil mixtures of Fig. 6. It can be noted that the Caprylic–EPA–Caprylic enriched palm oil curves are similar whatever the concentration but are very different from the pure palm oil curve. This is expected as the chemical structure of the mixture molecules is changed but it is meaningful because a single 5% Caprylic–EPA–Caprylic concentration shifts the DSC peaks significantly. However, as a whole, these curves are difficult to interpret in terms of properties.

Now, we compare the addition of 30% of four MLM structured lipids, Caprylic-X-Caprylic, with X being a LCFA: EPA (eicosapentaenoic acid–C20:5) as before, DHA (docosahexaenoic acid–C22:6), AA (arachidonic acid–C20:4) and γ–linolenic acid (6,9,12-octadecatrienoic acid–C18:3). Figure 8 represents the melting curves for these mixtures whereas Fig. 9 shows the related DSC curves.

The results indicate that the structured lipids with EPA, DHA and AA lower the melting points at −20 °C compared to pure palm oil, whereas the addition of γ-linolenic acid increases the melting point by +18 °C. Among these 4 fatty acids, the γ-linolenic has three double bonds (C18:3) while EPA, DHA and AA have five, six, and four

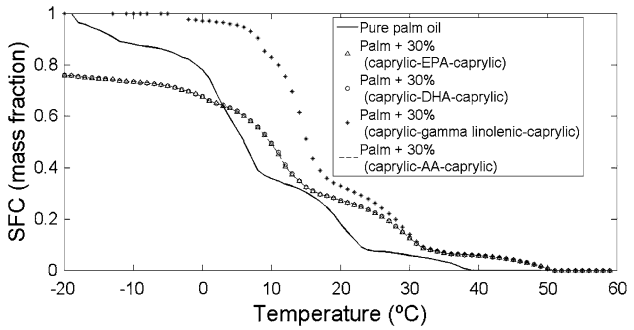

Fig. 8 Simulated melting curves for palm oil enriched with different structured lipids

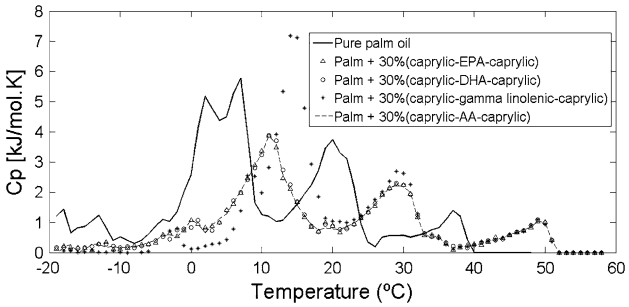

Fig. 9 Simulated DSC curves for the mixtures presented in Fig. 8

double bonds, respectively, resulting in very low melting points (−54, −44, and −49 °C, respectively). As a result, EPA, DHA and AA are all in the liquid phase at the beginning of the computation and the three relevant curves overlap. Therefore, the effect of decreasing SFC is more pronounced in the last ones. But pure palm oil still exhibits the lowest crystallization temperature. Therefore one notes that EPA, DHA and AA expand the melting range on both sides whereas γ-linolenic acid shifts it upwards.

Figure 9 shows the corresponding DSC simulations for the mixtures of Fig. 8. As in the previous case, the shape of the curves for the palm oil mixtures + SLs are very different from that of the pure palm oil and also there are differences among them, as the chemical structure of the mixtures is different for each curve.

Conclusions and Future Work

Crystallization and melting behavior play an important role in the fat-based products acceptance and quality requirements. These phenomena were modeled using a solid–liquid equilibrium framework coping with TAG polymorphism. Following the literature we considered the liquid phase and the unstable α solid phase as ideal whereas the β and β′ non-ideal behavior was modeled with the Margules activity coefficient model where the binary interaction parameters are predicted by using an isomorphism model. Solving is done by direct minimization of the Gibbs free energy using a generalized reduced gradient algorithm whose robustness has been assessed.

Such a modeling has been used earlier but on simple binary or ternary mixtures and always with parameter fitting of experimental data. Within the context of computer aided product design reverse engineering of new lipid based applications, the computer tool was used in a predictive manner to compute the melting range, the solid fat content vs temperature and the DSC curve from the knowledge of the TAG blends composition.

The tool was validated on experimental data available for a binary POP/PPP mixture, on a ternary MPM/SSO/OOO mixture, on pure palm oil and cocoa butter. There was a close qualitative agreement between predictions and experimental data available. In all cases the solid fat content quantitative agreement was achieved within 15%. It was pointed that some experimental data lacked uncertainty information, likely to exist as clear and softening points are sometimes difficult to assess when recording phase diagrams, or as DSC curves are heating rate dependent. Concerning palm oil, no comparison with other models was possible because none was found in the literature. Then the tool was used to predict the property changes when adding caprylic acid–X–caprylic acid to pure palm oil, with X being EPA (eicosapentaenoic acid–C20:5) as before, DHA (docosahexaenoic acid–C22:6), AA (arachidonic acid–C20:4) and γ-linolenic acid (C18:3). Those structured TAG belong to the important MLM class where the long chain fatty acids in position *sn*-2 may bring benefits for health.

Results showed that the lipid addition affected the SFC and the melting range even at a 5% concentration. At 30% concentration, EPA, DHA and AA expand the palm oil melting range on both sides whereas γ-linolenic acid shifts it upwards.

Work in preparation are heading in two directions. First the complete prediction of SFC and melting range from the fatty acid distribution instead of the TAG composition, with underneath the generation of the TAG themselves, using statistical models. Second, the development of a computer aided mixture and blend design framework for finding new structured lipids coping with target property values set a priori. In that case, the solid–liquid equilibrium tool can be supplemented with a rheological behavior prediction model, a detailed nutritional power evaluation model and many other properties that qualify them for a specific application.

Acknowledgments We acknowledge the financial support received from The National Council for Scientific and Technological Development (CNPq-Brazil), Coordenação de Aperfeiçoamento de Pessoal de Nível Superior (CAPES-Brazil) and the ALFA-II-400 FIPHARIA program (Europe).

Appendix: Margules Model and Binary Interaction Parameter models

The definition of the activity coefficient is given by the following Eq. [27]:

$$RT\ln\gamma_i(T,P,x) = \bar{g}_i^E = \left(\frac{\partial n g^E}{\partial n_i}\right)_{T,P,n_{j\neq i}} \tag{A1}$$

The two-suffix Margules model for multicomponent mixtures is given by:

$$g^E = \sum_{i=1}^{nc}\sum_{j=i+1}^{nc} A_{ij}x_i x_j \tag{A2}$$

where

$$A_{ij} = 2qa_{ij} \tag{A3}$$

The term q is a measure of the size of the molecules in the pair and $a_{ij}$are interaction parameters between molecules i and j. In the Margules equations is assumed that $q_i = q_j = q$ (molecules with similar size). However, it is used frequently for all sorts of mixtures, regardless of the relative sizes of the different molecules [27].

The work of Wesdorp [15] showed that there is a great correlation between the degree of isomorphism (coefficient of geometrical similarity) and the parameter A_{ij}. The degree of isomorphism between two TAG can be described by the following expression:

$$\varepsilon = 1 - \frac{v_{\text{non}}}{v_o} \tag{A4}$$

v_{non} is the sum of the absolute differences in carbon number of each of three chains and for v_0 the sum of the carbon numbers of the smallest chain on each glycerol position. Linear regression of experimentally determined A_{ij} parameters versus the calculated isomorphism as defined by Eq. A4 led to the following correlations [15]:

$$\varepsilon > 0.93: \frac{A_{ij}^{\beta'}}{RT} = 0 \text{ (highmolecular similarity, complete miscibility)} \tag{A5}$$

$$\varepsilon \leq 0.93: \frac{A_{ij}^{\beta'}}{RT} = -19.5\varepsilon + 18.2 \tag{A6}$$

$$\varepsilon > 0.98: \frac{A_{ij}^{\beta}}{RT} = 0 \text{ (highmolecular similarity, complete miscibility)} \tag{A7}$$

$$\varepsilon \leq 0.98: \frac{A_{ij}^{\beta}}{RT} = -35.8\varepsilon + 35.9 \tag{A8}$$

The primary value of the Margules equations lies in their ability to serve as simple empirical equations for representing experimentally determined activity coefficients with only a few constants and when, as is often the case, experimental data are scattered and scarce, they serve as an efficient tool for interpolation and extrapolation with respect to composition [27].

References

1. Jiménez-Colmenero F (2007) Healthier lipid formulation approaches in meat based functional foods. Technological options for replacement of meat fats by non-meat fats. Trends Food Sci Technol 18(11):567–578
2. Yang T, Zhang H, Mu H, Sinclair AJ, Xu X (2004) Diacylglycerols from butterfat: production by glycerolysis and short-path distillation and analysis of physical properties. J Am Oil Chem Soc 81(10):979–987
3. Osborn H, Akoh C (2002) Structured lipids-novel fats with medical, nutraceutical, and food applications. Compr Rev Food Sci Food Saf 3(1):93–103
4. Singh AP, McClements DJ, Marangoni AG (2004) Solid fat content determination by ultrasonic velocimetry. Food Res Int 37:545–555
5. Arifin N, Cheong LZ, Koh SP, Long K, Tan CP, Yusoff MSA, Aini IN, Lo SK, Lai OM (2009) Physicochemical properties and sensory attributes of medium-and long-chain triacylglycerols (MLCT)-enriched bakery shortening. Food Bioprocess Technol. doi:10.1007/s11947-009-0204-0
6. Pantzaris TP, Basiron Y (2002) The lauric (coconut and palm kernel) oils. In: Gunstone FD (ed) Vegetable oils in food technology: composition, properties and uses. Blackwell, Oxford, pp 157–202
7. Braipson-Danthine S, Deroanne C (2004) Influence of SFC, microstructure and polymorphism on texture (hardness) of binary blends of fats involved in the preparation of industrial shortenings. Food Res Int 37:941–948
8. Lee K, Akoh C (1998) Characterization of enzymatically synthesized structured lipids containing eicosapentaenoic, docosahexaenoic, and caprylic acids. J Am Oil Chem Soc 75(4):495–499
9. Timm-Heinrich M, Nielsen NS, Xu X, Jacobsen C (2004) Oxidative stability of structured lipids containing C18:0, C18:1, C18:2, C18:3 or CLA in *sn*2-position—as bulk lipids and in milk drinks. Innov Food Sci Emerg Technol 5(2):249–261
10. Iwasaki Y, Yamane T (2000) Enzymatic synthesis of structured lipids. J Mol Catal B Enzym 10(1–3):129–140
11. Ruxton CHS, Reed SC, Simpson MJA, Millington KJ (2004) The health benefits of omega-3 polyunsaturated fatty acids: a review of the evidence. J Hum Nutr Dietet 17:449–459
12. Shahidi F (2004) Functional foods: their role in health promotion and disease prevention. J Food Sci 69(5):146–149
13. Gani R (2004) Chemical product design: challenges and opportunities. Comp Chem Eng 28:2441–2457
14. Sato K (2001) Crystallization behaviour of fats and lipids—a review. Chem Eng Sci 56:2255–2265
15. Wesdorp LH, van Meeteren JA, de Jong S, Giessen RVD, Overbosch P, Grootscholten PAM, Struik M, Royers E, Don A, de Loos TH, Peters C, Gandasasmita I (2005) Liquid-multiple solid phase equilibria in fats. In: Marangoni AG (ed) Theory and experiments. Fat Crystal Networks, New York, pp 481–710
16. Inoue T, Hisatsugu Y, Yamamoto R, Suzuki M (2004) Solid–liquid phase behavior of binary fatty acid mixtures 1. Oleic acid/stearic acid and oleic acid/behenic acid mixtures. Chem Phys Lipids 127:143–152
17. Zhou Y, Hartel RW (2006) Phase behavior of model lipid systems: solubility of high-melting fats in low-melting fats. J Am Oil Chem Soc 83:505–511
18. Zhang L, Ueno S, Miura S, Sato K (2007) Binary phase behavior of 1, 3-dipalmitoyl-2-oleoyl-*sn*-glycerol and 1, 2-dioleoyl-3-palmitoyl-rac-glycerol. J Am Oil Chem Soc 84:219–227
19. Himawan C, Starov V, Stapley A (2006) Thermodynamic and kinetic aspects of fat crystallization. Adv Colloid Interface Sci 122(1–3):3–33
20. Won K (1993) Thermodynamic model of liquid-solid equilibria for natural fats and oils. Fluid Phase Equilibr 82:261–273
21. Slaughter DW, Doherty MF (1995) Calculation of solid-liquid equilibrium and crystallization paths for melt crystallization processes. Chem Eng Sci 50(11):1679–1694
22. Costa MC, Rolemberg MP, Boros LAD, Krahenbuhl MA, de Oliveira MG, Meirelles AJA (2007) Solid-liquid equilibrium of binary fatty acid mixtures. J Chem Eng Data 52:30–36
23. Bragg WL, Williams EJ (1934) The effect of thermal agitation on atomic arrangement in alloys. Proceedings of the Royal Society of London. Series A, Containing Papers of a Mathematical and Physical Character 145(855): p 699–730
24. Slaughter DW, Doherty MF (1995) Calculation of solid–liquid equilibrium and crystallization paths for melt crystallization processes. Chem Eng Sci 50(11):1679–1694
25. Abes M, Bouzidi L, Narine SS (2007) Crystallization and phase behavior of 1,3-propanediol esters II. 1,3-Propanediol distearate/1,3-propanediol dipalmitate (SS/PP) and 1,3-propanediol distearate/1,3-propanediol dimyristate (SS/MM) binary systems. Chem Phys Lipids 150:89–108
26. Boodhoo MV, Kutek T, Filip V, Narine SS (2008) The binary phase behavior of 1,3-dimyristoyl-2-stearoyl-*sn*-glycerol and 1,2-dimyristoyl-3-stearoyl-*sn*-glycerol. Chem Phys Lipids 154(1):7–18
27. Prausnitz JW, Lichtenthaler RN, de Azevedo GE (1998) Molecular thermodynamics of fluid phase equilibria. 3th edn. Prentice-Hall, New York
28. McDonald CM, Floudas CA (1997) GLOPEQ: a new computational tool for the phase and chemical equilibrium problem. Comp Chem Eng 21:1–23
29. Teles dos Santos M, Carrilo Le Roux GA, Joulia X, Gerbaud V (2009) Solid–liquid equilibrium modelling and stability tests for triacylglycerols tixtures. Comp Aided Chem Eng 27:885–890
30. Michelsen ML (1982) The isothermal flash problem Part I. stability. Fluid Phase Equilibr 9:1–19
31. Rosenthal RE (2008) GAMS Release 23.2. A user's guide. GAMS Development Corporation, Washington, DC
32. Takiyama H, Suzuki H, Uchida H, Matsuoka M (2002) Determination of solid–liquid phase equilibrium by using measured DSC curves. Fluid Phase Equilibr 194–197:1107–1117
33. Zéberg-Mikkelsen CK, Stenby EH (1999) Predicting the melting points and the enthalpies of fusion of saturated triglycerides by a group contribution method. Fluid Phase Equilibr 162:7–17
34. Ceriani R, Gani R, Meirelles AJA (2009) Prediction of heat capacities and heats of vaporization of organic liquids by group contribution methods. Fluid Phase Equilibr 28:49–55
35. Bruin S (1999) Phase equilibrium for food product and process design. Fluid Phase Equilibr 158–160:657–671
36. Sambanthamurthi R, Sundram K, Tan Y (2000) Chemistry and biochemistry of palm oil. Prog Lipid Res 39:507–558
37. Lin SW (2002) Palm oil. In: Gunstone FD (ed) Vegetable oils in food technology: composition properties and uses. Blackwell, Oxford, pp 59–97
38. Keller G, Lavigne F, Loisel C, Ollivon M, Bourgaux C (1996) Investigation of the complex thermal behaviour of fats. J Therm Anal 47:1545–1565
39. Sato K, Koyano T (2001) Crystallization properties of cocoa butter. In: Garti N, Sato K (eds) Crystallization processes in fats and lipid systems. Marcel Dekker, New York, pp 429–456